Макрогетероциклы
http://macroheterocycles.isuct.ru

DOI: 10.6060/mhc2012.121197v

Effect of Cyanine Dyes on Photoelectric, Nonlinear Optical and Photorefractive Properties of Composites Based on Carbon Nanotubes

Anatoly V. Vannikov,[a@] Antonina D. Grishina,[a] Andrej S. Laryushkin,[a] Tatyana V. Krivenko,[a] Vladimir V. Savel'ev,[a] and Rodney W. Rychwalski[b]

Dedicated to Academician Aslan Tsivadze on the occasion of his 70th Anniversary

[a]*A.N. Frumkin Institute of Physical Chemistry and Electrochemistry, Russian Academy of Sciences, 19991 Moscow, Russia*
[b]*Department of Materials and Manufacturing Technology, Chalmers University of Technology, SE_41296, Goteborg, Sweden*
[@]*Corresponding author E-mail: van@elchem.ac.ru; anatoly.vannikov@rambler.ru*

Analysis of photoelectrical, nonlinear optical, and photorefractive properties of composites PVK containing single-walled carbon nanotubes shows that addition of visible range cyanine dye with high electron affinity into the composites provides considerable increase of quantum efficiency of the mobile charge carries generation at 1064 nm, but reduces the third order susceptibility. As a result, photorefractive gain coefficient Γ of object laser beam increases twofold and achieves after pre-illumination the value 120 cm^{-1}.

Keywords: Quantum efficiency, third order susceptibility, photorefractive gain coefficient.

Влияние цианиновых красителей на фотоэлектрические, нелинейно–оптические и фоторефрактивные свойства композитов на основе углеродных нанотрубок

А. В. Ванников,[a@] А. Д. Гришина,[a] А. С. Ларюшкин,[a] Т. В. Кривенко,[a] В. В. Савельев,[a] Р. В. Ричвальски[b]

Посвящается академику А. Ю. Цивадзе по случаю его 70–летнего юбилея

[a]*ФГБУН Институт физической химии и электрохимии им. А.Н. Фрумкина РАН, 119991 Москва, Россия*
[b]*Department of Materials and Manufacturing Technology, Chalmers University of Technology, SE_41296, Гетеборг, Швеция*
[@]*E-mail: van@elchem.ac.ru; anatoly.vannikov@rambler.ru*

Анализ фотоэлектрических, нелинейно-оптических и фоторефрактивных свойств композитов из поливинилкарбазола, содержащих одностенные углеродные нанотрубки, показал, что добавление цианинового красителя видимого диапазона с высоким электронным сродством приводит к значительному увеличению квантовой эффективности генерации подвижных носителей заряда при 1064 нм, но снижает восприимчивость третьего порядка. В результате коэффициент фоторефрактивного двулучевого усиления объектного лазерного луча возрастет в два раза и достигает 120 см$^{-1}$.

Ключевые слова: Квантовая эффективность, нелинейная восприимчивость третьего порядка, фоторефрактивный коэффициент усиления.

Introduction

Photoelectric, nonlinear optical and photorefractive characteristics at 1064 nm are discussed for composites of polyvinylcarbazole (PVK) containing closed single-walled carbon nanotubes (SWCNT) with an additive of visible range cyanine dye with high electron affinity. Photorefractive effect arises in materials which possess simultaneously photoelectric and nonlinear optical properties. SWCNT acts as spectral sensitizers toward laser irradiation at 1064 nm and the third order nonlinear optical chromophores. This work continues direction of investigations of photorefractive materials on the basis of unplasticized polymers with a high glass transition temperature T_g (for PVK T_g = 200 °C) in which the random orientation of chromophores obtained upon layer casting is frozen. A high glass transition temperature improves the stability of characteristics of the material, but requires using nano-dimensional nonlinear optical chromophores with considerable third order nonlinearity.[1] Indeed, in unplasticized polymers, an electric field does not provide the chromophores orientational polarization; the nonlinear second-order susceptibility $\chi^{(2)} = N f^3 \beta \langle \cos^3 \xi \rangle$ is zero, as in the case of random distribution of nonlinear chromophores the mean value of $\langle \cos 3\xi \rangle = 0$. (Here N is the chromophore concentration, β is the second order molecular polarizability, ξ is the angle between the principal chromophore axis and the direction of the polarizing electric field and $f = (n_0 + 2)/3$ is the Lorentz factor, for PVK n_0 = 1.5). Simultaneously the third-order dielectric susceptibility has a nonzero value:

$$\chi^{(3)} = N\gamma f^4 \langle \cos^4 \xi \rangle,$$

that is the mean value of $\langle \cos^4 \xi \rangle = 1/5$ at a random distribution of orientation angles ξ. (Here γ is the third-order molecular polarizability). The quantity γ is low for short nonlinear optical chromophores but increases as $\gamma \sim l^{2.36}$ with the increase in the conjugation length l[2,3] or in the length of cooperative electronic excitation.[4,5] Thus, a necessary condition for the preparation of effective photorefractive materials from unplasticized polymers with a high T_g value is the use of nanosized structures, in particular, carbon nanotubes (CNT). Photorefractive polymer composites based on non-oxidized and oxidized closed single-wall nanotubes[6-12] and also multi-wall carbon nanotubes[13] were studied earlier.

Experimental

Electronic absorption spectra of the polymer composites were recorded on a Shimadzu UV-3101PC spectrophotometer in tetrachloroethane (TCE) solution or in layers applied on a quartz plate. Method of *z*-scanning on the basis of femtosecond laser was used for estimation of the third order nonlinearity.

To prepare composites, SWNTs were first dispersed in TCE for 30 min using an UZDN-A ultrasonic powder dispenser. Then, Dye **1** – 3,3'-diethylthiatricarbo-cyanine iodide or Dye **2** – 1,1'-diethyl-4,4'-dicarbocyanine iodide was added in the solution.

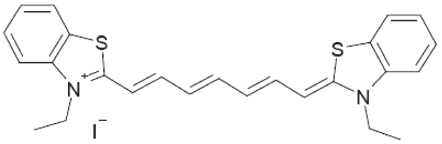

Dye **1**: λ_{max} = 760 nm and the longwave limit in the range of 850 nm, electrochemical reduction potential is E_{red} = – 0.78 V and oxidation potential E_{ox} = 0.28 V vs. saturated calomel electrode (SCE).

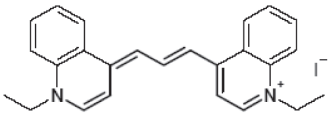

Dye **2**: λ_{max} = 571 nm, E_{red} = –1.17 V and E_{ox} = 0.90 V (SCE). As Fermi level of SCE is separated from vacuum zero level on 4.64 eV, therefore LUMO levels correspond to 3.86 eV for Dye **1** and 3.47 eV for Dye **2**.

The obtained solution was stored for 24 h. For this time, the optical absorption of Dye **1** has decreased from 1.4 to 0.2 due to adsorption Dye **1** on SWCNTs. Then, PVK in TCE was added to the dispersion solution and the viscous mixture was again subjected to 5 min ultrasonic treatment.

The measurement cells were prepared as follows: first, in order to decrease the dark current, a dielectric Al_2O_3 film was sputtered on the ITO electrode superimposed on glass support. Then a polymer composition solution was poured onto it. It was dried for a prolonged period at 60-90 °C. Then, after the solvent was evaporated, the upper glass-ITO electrode was pressed to the layer. At measurements of photoelectric characteristics, the polymer layer was illuminated by a single laser beam from the side of a transparent ITO electrode and the second electrode used was a nontransparent silver paste.

The basic measurements were performed for the composites of PVK and SWCNTs of 0.26 wt. % and a dye of 0.3 wt. %. As the SWNT content is increased to 0.43 wt. %, the dark current grows considerably by a factor of a few tens, thus complicating the determination of photocurrent in such samples.

Results and Discussion

Photoelectric Characteristics

SWNTs are responsible for optical absorption over the entire visible and near IR range - from ~500 to 2000 nm. The dependence of the quantum efficiency for the formation of mobile charge carriers on the applied field E_0 at 1064 nm was determined from the field dependence of photocurrent $J_{ph}(E_0)$. The photocurrent was determined as the difference between the current during illumination ($J_{ph} + J_d$) and in dark J_d: $J_{ph} = (J_{ph} + J_d) - J_d$. Figure 1 shows the dependence of the quantum efficiency for the formation of mobile charge carriers on the applied field $\vartheta(E_0)$ which was determined from the field dependence of photocurrent $J_{ph}(E_0)$ according to the equation.

$$\vartheta(E_0) = J_{ph}(E_0) h\nu / e[I_0(1 - \exp(-\alpha_0 d))]. \qquad (1)$$

Here, at λ = 1064 nm, the value of $h\nu$ = 1240/1064 = 1.165 eV; I_0 = 5.2 W/cm^2 is the intensity of laser radiation incident on the layer. Layer thickness d = 12 μm. The absorbance at 1064 nm is A = 0.005 and, therefore, $\alpha_0 = 2.3A/d = 9.6$ cm^{-1}. The value of $(1 - \exp(-\alpha_0 d))$ is the fraction of the light energy absorbed in the layer.

The solid curves in Figure 1 are accorded with Onsager equation $\vartheta(E_0) = \phi_0 \times P(r_0, E_0)$, where ϕ_0 is the quantum yield of thermalized electron–hole pairs with the initial separation radius being r_0; $P(r_0, E_0)$ is the probability that charges in

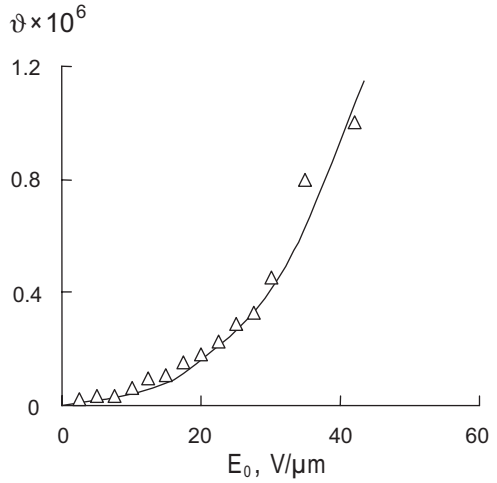

Figure 1. Dependences of quantum efficiency ϑ on applied field E_0 in the composite PVK/SWCNT 0.26 wt. %/Dye 1 0.3 wt. %.

pairs will escape recombination at the separation radius of r_0:[14]

$$P(r_0, E_0)= \exp(-r_c/r_0)\{[1 + (r_c/r_0)(eE_0r_0/2kT) - (r_c/r_0)K_1(eE_0r_0/2kT)^2 + (r_c/r_0)K_2(eE_0r_0/2kT)^3 - (r_c/r_0)K_3(eE_0r_0/2kT)^4]\} \quad (2)$$

here $K_1 = [2 - (r_c/r_0)]/3$; $K_2 = [1 - (r_c/r_0) + (r_c/r_0)^2/6]/2$; $K_3 = [2 - 3(r_c/r_0) + (r_c/r_0)^2 - (r_c/r_0)^3/12]/15$.

The Coulomb radius $r_c = e^2/4\pi\varepsilon\varepsilon_0 kT$ equal to 190 Å is the radius at which the mutual Coulomb electron-hole attraction in the pair equals kT for $\varepsilon = 3$ at room temperature, $\varepsilon_0 = 8.85\cdot10^{-14}$ F/cm.

The Onsager formalism was applied in work[15] to PVK doped with various acceptors. It was shown that relaxed charge-transfer states with $r_0 \leq 10$ Å are precursors of free carriers.

It was shown previously[12] for the composite in absence of any dye the quantum efficiency of the mobile charge carriers generation is closely fitted with the Onsager Equation 2 expanded up to E_0^4. The quantum yields ϕ_0 = 0.08 if we take r_0 = 9.8 Å.[12] These results were transcribed in the present work. In the presence of Dye 1 0.3 wt. % field dependence of the quantum efficiency is well fitted with the Onsager Equation 2 expanded up to $E_0^3 r_0$=10.5 Å and ϕ_0 = 0.5 (solid curve *2* in Figure 1). An increase in the photocurrent and quantum efficiency of mobile charge carriers generation after addition of Dye 1 can be explained by formation of initial $PVK^{+\bullet}$…$SWCNT^{-\bullet}$ pairs as a result of photoexcitation of SWCNTs. These initial pairs are partially divided on free charges or recombine.

Retrapping of electron by Dye 1 from $SWCNT^{-\bullet}$ considerable increases photocurrent and quantum efficiency (Figure 1) due to the increase of the initial separation radius r_0 from 9.8 Å to 10.5 Å and quantum yield from 0.08 to 0.5.

As opposed to the effect of Dye 1, introduction of Dye 2 into the composition does not result in the increase of photocurrent and quantum efficiency. This is possibly due to the marked above increase in the LUMO level on 0.4 V at a transition from Dye 1 to Dye 2. Work function of SWCNT estimates generally as 5 eV.[16] The level of photo excited SWCNT is near to 5 – 1.17 = 3.83 eV. Hence, retrapping of electron from $SWCNT^{-\bullet}$ is a process energetically advantageous for Dye 1 but an activation hindered transition for Dye 2.

Nonlinear Optical Characteristics Composites PVK/SWCNT with and without Dye

A *z*-scanning setup on the basis of a pulsed femtosecond laser made according to the type shown in Figure 2 was used for measurement of the third order susceptibility $\chi^{(3)}$.[17] The basic elements of the setup are a pulsed femtosecond laser Origami-10 (*1*) irradiating at wavelength λ = 1030 nm. The laser beam was focused by lens (*2*) with the focal distance of 6.5 cm. The beam radius and light intensity in the lens focus were w_0 = 17 μm and $6.93\cdot10^8$ W/cm^2 in one pulse. A slide unit allowed moving (*z*-scanning) sample (*3*) along the laser beam from the prefocal region (–*z*) to lens focus (*z* = 0), and next to postfocal region (+*z*). The light transmission was measured by photodetector in two modes: with diaphragm *4* (with an aperture of 0.1 cm at the diaphragm center) put on the photodetector (closed aperture mode, T_{CA}) and without a diaphragm (open aperture mode, T_{OA}). The signal from photodetector was enhanced and registered by a memory oscilloscope connected to a computer. Due to high light intensity in the focal range, nonlinear optical effects appeared. As the sample is moving from -z to z = 0, the refractive index

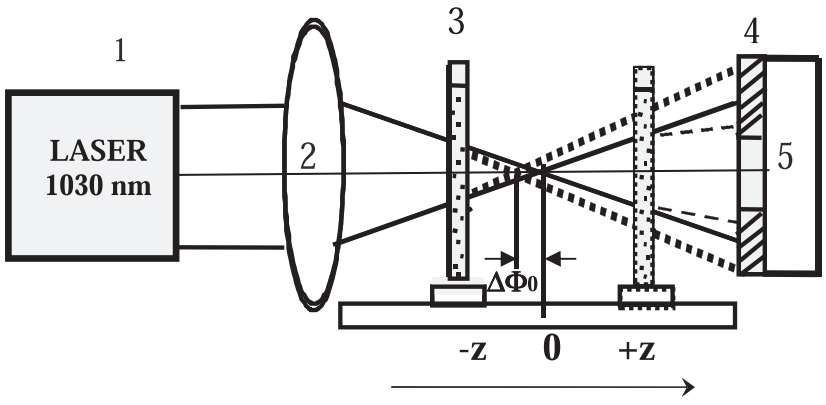

Figure 2. *Z*-scanning setup. (*1*) femtosecond laser (1030 nm), (*2*) focusing lens, (*3*) moving sample, (*4*) diaphragm with an aperture of 1 mm, and (*5*) photodetector.

grows from the linear value of n_0 (for PVK, $n_0 = 1.5$) to the value:

$$n = n_0 + n_2 I_0,$$

and so the sample acts as added lens. As shown in Figure 2, it provides phase distortion $\Delta\Phi_0$, *i.e.* shifts the focus to the prefocal region.

Figure 3a,b presents the dependence of T_{CA} on the distance from the focus ($z = 0$) in a solid composite PVK/SWCNTs 0.26 wt. % (curve *1*, Figure 3a), in quartz substrate (line *2*, Figure 3a) and in solid composite PVC/SWCNTs 0.26 wt. %/Dye 1 0.3 wt. % (Figure 3b). The experimental points of T_{CA} on z were fitted with the theoretical relationship:[18]

$$T_{CA} = 1 - 4\Delta\Phi_0 x/[(x^2 + 1)(x^2 + 9)] \quad (3)$$

by choosing phase distortion $\Delta\Phi_0$ Here, $x = z/z_0$ is the relative distance from the sample to the focus, $z_0 = n_0\pi w_0^2/\lambda$ is the Rayleigh region, which, as known,[19] is the distance from the focus to positions at which the beam radius is $w_0 \cdot (2)^{0.5}$. Value $\Delta\Phi_0$ related to the nonlinear effect by the relationship of

$$n_2 I_0 = \Delta\Phi_0 \lambda/2\pi L_{eff} \quad (4)$$

$L_{eff} = (1 - e^{-\alpha 0 L})/\alpha_0$, $L = 60$ μm is the composite thickness; and $\alpha_0 = 1.15$ cm^{-1} is optical absorption at 1030 nm. Hence, $L_{eff} = 0.0059$ cm. The solid curve in Figure 3a is the dependence (3) at $\Delta\Phi_0 = 3.5$. As follows from relationship (4), $n_2 I_0 = 0.0096$ and $n_2 = 9.4 \cdot 10^{-12}$. The real part of the third order susceptibility is related to n_2 by the relationship:

$$\chi^{(3)} = n_2 \times (n_0^2/0.0394) \text{ esu.}$$

Therefore, in the composite of PVK and SWCNTs 0.26 wt. %, real $\chi^{(3)} = 5.4 \cdot 10^{-10}$ esu.

Figure 3b shows that the $\Delta\Phi_0$ value decreases fivefold (from $\Delta\Phi_0 = 3.5$ to $\Delta\Phi_0 = 0.7$) after addition of Dye 1 0.3 wt. % in the composite of PVK and SWCNTs 0.26 wt. %, apparently due to the opposite orientation of dipoles of Dye 1 and SWCNT at adsorption of Dye 1 on the nanotube.

The third order susceptibility was also measured in dispersions of 0.1 and 0.2 mg of SWCNT in 1 ml of TCE after sonication for 30 min. The value $\Delta\Phi_0$ does not change by increasing the time of intense irradiation in the focal region from 40 μs to 450 μs, thereby indicating a significant excess of third order susceptibility over the thermo-optical effect. Relationship 3 fits the experimental points at $\Delta\Phi_0 = 2.2$ for 0.1 mg of SWCNT/1 ml of TCE and at $\Delta\Phi_0 = 4.2$ for 0.2 mg of SWCNT/1 ml of TCE. Thus, taking into account the measurement error, we can assume that the phase distortion $\Delta\Phi_0$ is largely determined by the amount of SWCNT. Therefore, the real component of the third order susceptibility for 0.2 mg of SWCNT/1 ml of TCE can be estimated as $\chi^{(3)} = 0.57 \cdot 10^{-10}$ esu. This value is somewhat higher than the value measured in composite 1g PVK/0.2 mg SWCNTs in which susceptibility takes value $\chi^{(3)} = 0.4 \cdot 10^{-10}$ esu. This effect is presumably due to the known strong interaction of nanotube charges and polymer semiconductors,[20] which hinders the nonlinear polarization.

So, the addition of Dye **1** 0.3 wt. % into composite PVK/SWCNT 0.26 wt. % provides the multiple increase of quantum efficiency and the fivefold decrease of third order dielectric susceptibility. It follows thence that photorefractive effect will increase under such relationships.

Photorefractive Characteristics

The PR characteristics were measured on a holographic device by the two-beam coupling technique using linearly polarized radiation from a continuous Nd:YAG laser (1064 nm). The beams intersected at an angle of $2\theta = 15°$ in polymer

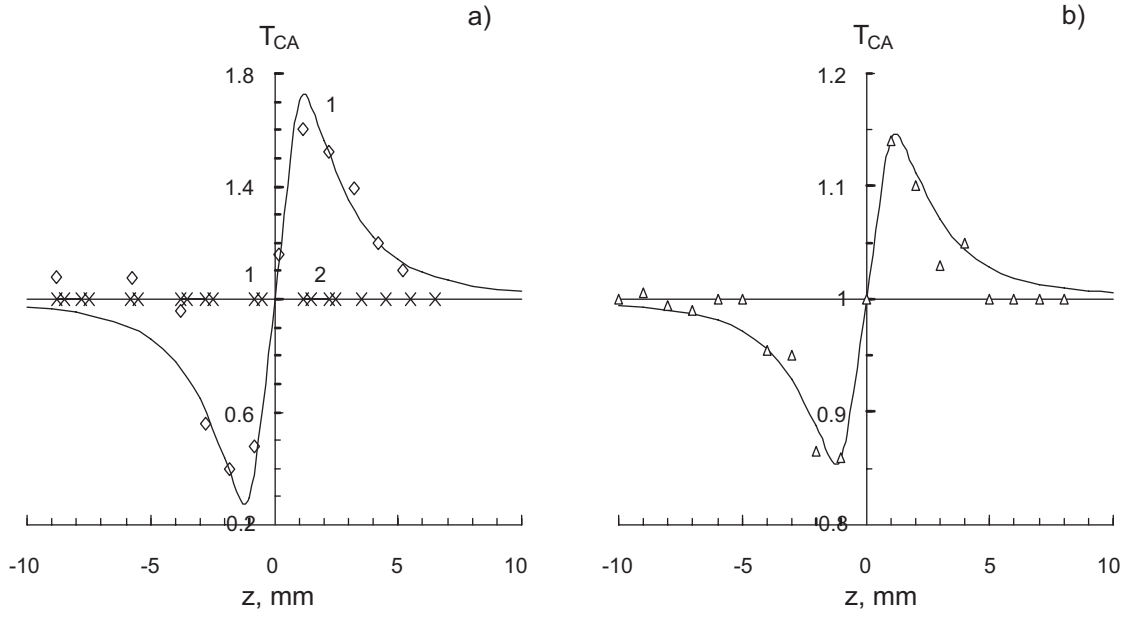

Figure 3. Dependence of T_{CA} on the distance from the focus ($z = 0$) in solid composite PVK/SWCNTs 0.26 wt. % (curve *1*), in quartz substrate (line *2*) (*a*) and in solid composite PVK/SWCNTs 0.26 wt. %/Dye 1 0.3 wt. % (*b*). Composite thickness $L = 60$ μm.

composite. The bisector of this angle formed an angle of φ = 45° with the cell surface. The measurement geometry was such that beam 2 was amplified and beam 1 was attenuated at a negative potential on the electrode for the outgoing beams (exit electrode) but beam 2 was attenuated and beam 1 was amplified when a positive voltage was applied to the exit electrode. The diameter of the beam intersection area was 3 mm.

Photorefractive effect involves the formation of the two-beam interference pattern in the polymer layer, the photogeneration of the electron–hole pairs in the bright regions, drift of the charges in the applied dc electric field E_0 to dark regions, and trapping. The trapped electrons and holes produce the periodic space-charge field E_{sc}. Field (E_0+E_{sc}) induces electron third order polarization of the nonlinear optical chromophores and thereby form periodic modulation of the index refraction, *i.e.* diffraction grating $\Delta n = (2\pi/n)\chi^{(3)}(E_0 + E_{sc})^2$. Necessary condition for the forming of the photorefractive effect is different mobilities of unlike charges, the trapping of less mobile carriers of one sign near their formation sites and the drift of the more mobile oppositely charged carriers in a field E_0 toward dark fringes until their capture in deep traps. The holes are mobile charged carriers in PVK. Under these conditions, the field E_{sc} and, hence, the diffraction grating become displaced by a phase -ψ relative to interference fringes. A part of beam 1 (referent beam) reflected from the diffraction grating coincides in phase and direction with transmitted beam 2, which propagates from the interference fringe to the diffraction grating, and their constructive interference leads to an amplification of the intensity of beam 2 (information beam). The two beam coupling gain coefficient equals

$$\Gamma = 4\pi\Delta n\cos 2\theta \sin|\psi|/\lambda \qquad (5)$$

The reflected portion of beam 2 also coincides in direction with beam 1 but propagates in antiphase, thus providing destructive interference of the beams and a decrease in the intensity of beam 1. Reversion of E_0 direction initiates a change in the grating position (phase shift turns from the -ψ to the +ψ position) ensured by the corresponding change in the direction of charge transport. Under these conditions, beam 1 is amplified and beam 2 is attenuated.

The ability to amplify IR laser radiation makes photorefractive materials promising for various photonics applications. Photorefractive materials responsive to near-IR radiation at wavelength 1064 nm can be used in medical diagnostics of living tissues. A highly sensitive photorefractive device makes it possible to generate 3D holographic imaging of living tissues. Biological tissues strongly scatter radiation over the entire visible range but they are fairly transparent in the near IR region. For the purpose of use in biomedical studies, polymer composites possessing PR sensitivity at 830 nm, in region of action of a titanium-sapphire laser, were synthesized.[21] The transparency of tissues increases with an increase in the wavelength of electronic absorption, and InGaAs/GaAs multiple quantum well devices sensitive to 1064 nm were proposed as more promising for biomedical imaging.[22] These systems are costly and have restricted photorefractive characteristics; thus, the design of inexpensive polymer composites with high photorefractive properties that exhibit the photorefractive sensitivity at 1064 nm and longer wavelengths is a topical problem.

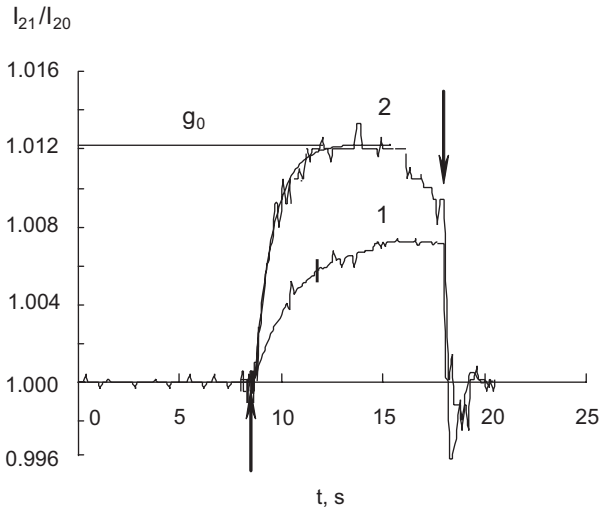

Figure 4. Kinetic curves of beam 2 amplification as a result two beam interaction for the PVK/SWCNT 0.26 wt % (*1*) and PVK/SWCNT 0.26 wt. %/Dye 1 0.3 wt. % (*2*) composites. Applied electric field E_0 = 83.3 V/μm.

Figure 4 shows amplification of information beam 2 as a result of two beam interaction with pump beam 1. The curves were measured in the field of E_0 = 83.3 V/μm and laser input radiation $I_1(0) = I_2(0) = 0.12$ W/cm^2 for the PVK/SWCNT 0.26 wt. % and PVK/SWCNT 0.26 wt. % Dye 1 0.3 wt. % polymer composites.

The following procedure was used to record two-beam coupling curves: first, beam 2 was switched on and its intensity I_{20} at the exit from the cell was measured; next, a negative voltage was applied to the exit electrode, the intensity of beam 2 did not vary under these conditions. A few seconds later (at a time $t = t_0$), beam 1 was successively switched on and off (upward and downward arrows, respectively, in Figure 4). As shown in Figure 4 the intensity of beam 2, I_{21}, grew to a maximal value after switching beam 1 on and took the initial value I_{20} after switching beam 1 off. Presented in Figure 4 a relative rise in intensity of beam 2 with time after switching beam 1 on may be represented by the expression:

$$I_{21}/I_{20} = 1 + (g_0 - 1)\{1 - \exp[-(t - t_0)/\tau]\} \qquad (6)$$

Here, g_0 is the gain factor (or the ratio I_{21}/I_{20} in maximum curve) and τ is the grating formation time constant or the response time of composite to two-beam exposure.

As seen in Figure 4, introduction of the Dye 1 into the PVK/SWCNT composite provides a nearly double increase in gain factor g_0 (curve *2*). The parameters of curves measured at E_0 = 83.3 V/μm and $I_1(0) = I_2(0) = 0.12$ W/cm^2 correspond to g_0 = 1.006 and τ = 2 s (curve 1) for composites without Dye 1 and g_0 = 1.012 and τ = 0.9 s (curves *2*) for composite containing Dye 1 0.3 wt. %.

Additional procedure - pre-illumination is used before photorefractive measurements and consists in illumination of the polymer layer with continuous light from a He–Ne laser (633 nm) in the region of optical absorption of Dye 1.

Photoexcitation of Dye 1 leads to the appearance of holes in PVK. It is assumed that these holes fill deep traps (the polymer end groups, carbazolyl dimers, *etc*.) and restrict their influence on the transport of holes generated under the conditions of the subsequent writing of a photorefractive grating. Pre-illumination of this sample results in an additional increase in gain factor and reduction in response time to values $g_0 = 1.024$ and $\tau = 0.4$ s.

Figure 4 shows also that intensity I_{21} first grows and reaches maximum and then decreases in the dye-containing sample. The decrease may be related to a decrease in constant field E_0 within the sample as a result of accumulation of space charge due to dark current.[23] To limit the residual action of space charge, the photorefractive curves were successively recorded for opposite polarities of the electrodes. At a change in the direction of the applied field to the opposite (the anode and cathode are interchanged), the intensity of beam *2* was attenuated according to the relationship of $I_{21}/I_{20} = 1 - (g_0 - 1)\{1 - \exp[-(t - t_0)/\tau]\}$; simultaneously, beam *1* was amplified. This change points uniquely to the photorefractive nature of the effect.

The beam coupling gain coefficient Γ is related to the beam coupling ratio g_0 by the equation

$$\Gamma L = \ln[\beta g_0/(1+ \beta - g_0)] \qquad (7)$$

Here $L = d/\cos(\varphi - \theta)$ is beam 2 optical path, $\beta = I_1(0)/I_2(0)$is ratio of input beams.

As follows from the data of Figure 5, the two beam gain coefficient equals $\Gamma = 80$ cm^{-1} at field $E_0 = 100$ V/μm and $I_1(0) = I_2(0) = 0.24$ W/cm^2. After pre-illumination gain coefficient and net gain coefficient grow to $\Gamma = 120$ cm^{-1} and $\Gamma - \alpha = 110.4$ cm^{-1}, respectively.

Figure 6 shows that the two beam gain coefficient grows according to growth of ratio $\beta = I_1(0)/I_2(0)$ at $\beta \le 2$. Initial growth of gain coefficient has a practical significance as allows correcting the veiled images. Indeed, at projection of the slide having veiled areas and hence transmitting beams with $I_2(0) < I_1(0)$ through the photorefractive polymer

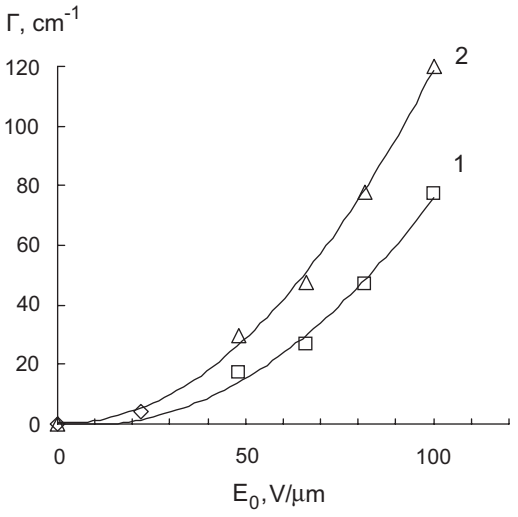

Figure 5. The field dependences of the two beam gain coefficient Γ at $I_1(0) = I_2(0) = 0.24$ W/cm^2 measured without (*1*) and with pre-illumination (*2*).

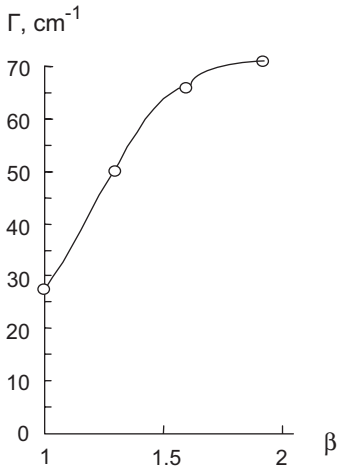

Figure 6. The dependence of two beam gain coefficient Γ on $\beta = I_1(0)/I_2(0)$ at $E_0 = 65$ V/μm and $I_1(0) = 0.24$ W/cm^2.

composite, the output image is corrected due to increase of gain coefficient (Figure 6).

Conclusions

Analysis of nonlinear optical, photoelectrical and photorefractive properties has shown, that at addition Dye 1 0.3 wt. % in composite PVK/SWCNT 0.26 wt. %

– third order susceptibility decreases in 5 times: from $\chi^{(3)} = 5.4 \cdot 10^{-10}$ esu to $1.1 \cdot 10^{-10}$ esu apparently due to the opposite orientation of dipoles of Dye 1 and SWCNT at adsorption of Dyes 1 on the nanotubes,

– quantum efficiency of the mobile charge carries generation increases in 14 times due to the increase of the initial separation radius r_0 from 9.8 Å to 10.5 Å and quantum yield from 0.08 to 0.5,

– as a result of countermovement of third order susceptibility and quantum efficiency of the mobile charge generation the photorefractive gain coefficient increases twofold and achieves $\Gamma = 120$ cm^{-1} after pre-illumination.

Acknowledgements. This work was financially supported by the Russian Foundation for Basic Research (project no. 11-03-00260) and Swedish Foundation for Strategic Research.

References

1. Vannikov A.V., Grishina A.D. *Russ. Chem. Rev*. **2003**, *72*, 471-488.
2. Knoester J. *Chem. Phys. Lett.* **1993**, *203*, 371-377.
3. Kusyk M.G. *Phys. Rev. Lett.* **2000**, *85*, 1218-1221.
4. Shelkovnikov V.V., Markov R.V., Plekhanov A.I., Simanchuk A.E., Ivanova Z.M. *High Energy Chem.* **2002**, *36*, 260-265.
5. Zhou H.S., Watanabe T., Mito A., Honma I., Asai K., Ishigure K., Furuki M. *Mat. Sci. Eng. B* **2002**, *95*, 180-185.
6. Vannikov A.V., Ryshwalski R.W., Grishina A.D., Pereshivko L.Ya., Krivenko T.V., Savel'ev V.V., Zolotarevskii V.I. *Opt. Spektrosk.* **2005**, *99*, 672-677.
7. Licea-Jimenes L., Grishina A.D., Pereshivko L.Ya., Krivenko T.V., Savelyev V.V., Rychwalski R.W., Vannikov A.V. *Carbon* **2006**, *44*, 113-120.

8. Grishina A.D., Licea-Jimenes L., Pereshivko L.Ya., Krivenko T.V., Savel'ev V.V., Rushwalski R.W., Vannikov A.V. *High Energy Chem*. **2006**, *40*, 341-347.
9. Grishina A.D., Pereshivko L.Ya., Licea-Jimenes L., Krivenko T.V., Savel'ev V.V., Rychwalski R.W., Vannikov A.V. *High Energy Chem.* **2007**, *41*, 267-273.
10. Vannikov A.V., Grishina A.D. *High Energy Chem.* **2007**, *41*. 162-175.
11. Grishina A.D., Pereshivko L.Ya., Licea-Jimenes L., Krivenko T.V., Savel'ev V.V., Rychwalski R.W., Vannikov A.V. *High Energy Chem.* **2008**, *42*, 378-384.
12. Vannikov A.V. Grishina A.D., Rychwalski R.W. *Carbon* **2011**, *49*, 311-319.
13. Grishina A.D., Licea-Jimenes L., Pereshivko L.Ya., Krivenko T.V., Savel'ev V.V., Rychwalski R.W., Vannikov A.V. *Polymer Science, Ser. A*. **2008**, *50*, 985-991.
14. Mozumder A. *J. Chem. Phys*. **1974**, *60*, 4300-4305.
15. Braun Ch.L. *J. Chem. Phys.* **1984**, *80*, 4157-4161.
16. Du Pasquier A., Unalan H.E., Kanwal A., Miller S., Chhowalla M. *Appl. Phys. Lett.* **2005**, *87*, 203511-203514.
17. Gnoli A., Razzari L., Righini M. *Optics Express* **2005**, *13*, 7976-7981.
18. Sheik-Bahae M., Said A.A., Wei T.-H., Hagan D.J., Van Stryland E.W. *IEEE J. Quantum Electron.* **1990**, *26*, 760-769.
19. Sutherland R.L. *Handbook of Nonlinear Optics.* New-York: Marcel Dekker, **1996**, p. 3.
20. Dalton A.B., Coleman J.N., Panhuis M.I.H., McCarthy B., Drury A., Blau A., Paci B., Nunzi J.M., Byrne H.J. *J. Photochem. Photobiol., A* **2001**, *144*, 31-35.
21. Kippelen B., Marder S.R., Hendrickx E., Maldonado J.L., Guillemet G., Volodin B.L., Steele D.D., Enami Y., Sandalphon, Yao Y.J., Wang J.F., Röckel H., Erskine L., Peyghambarian N. *Science* **1998**, *279*, 54-57.
22. Yu P., Balasubramanian S., Ward T.Z., Chandrasekhar M., Chandrasekhar H.R. *Synth Met.* **2005**, *155*, 406-409.
23. Borsenberger P.M., Weiss D.S. *Organic Photoreceptor for Xerography.* New York: Marcel Dekker, **1998**.

Received 20.11.2012
Accepted 03.12.2012